

EFFECT OF CRYSTALLINITY ON THE THERMAL EVOLUTION OF $\gamma\text{-Fe}_2\text{O}_3$

M. MACIAS¹, J. MORALES, J.L. TIRADO and C. VALERA

Dept°. Química Inorgánica e Ingeniería Química, Facultad de Ciencias,
Universidad de Córdoba, 14004 Córdoba, Spain

¹ Dept°. Química Inorgánica, Universidad de Sevilla

ABSTRACT

The thermal behaviour of $\gamma\text{-Fe}_2\text{O}_3$ samples of different pre-history is studied. This material is obtained from the following parent compounds, $\gamma\text{-FeOOH}$, $\alpha\text{-FeOOH}$, Fe_3O_4 , FeOOCH_3 and $\text{N}_2\text{H}_5\text{Fe}(\text{N}_2\text{H}_3\text{-COO})_3\cdot\text{H}_2\text{O}$. The temperature of the $\gamma\rightarrow\alpha\text{-Fe}_2\text{O}_3$ transformation is not clearly dependent on BET surface area or particle size. Small, platelike particles show a higher reaction rate, due to compaction possibilities. The lattice distortions in $\gamma\text{-Fe}_2\text{O}_3$ also induce an easier conversion into $\alpha\text{-Fe}_2\text{O}_3$.

INTRODUCTION

The development of new preparation procedures and the study of the thermal stability and magnetic properties of polycrystalline $\gamma\text{-Fe}_2\text{O}_3$ are the subject of continuous research work, mainly due to the applicability of this material in the preparation of magnetic supports of information. In this way, Rousset et al. [1-4] have pointed out that specific surface has a significant effect on the parameters of the thermal transformation $\gamma\text{-Fe}_2\text{O}_3 \rightarrow \alpha\text{-Fe}_2\text{O}_3$. Thus, a direct relationship between BET surface and transformation temperature was found by these authors. However, recent data of $\gamma\text{-Fe}_2\text{O}_3$ samples [5] obtained by thermal and mechanochemical decomposition of $\gamma\text{-FeOOH}$ are not in agreement with those conclusions. Instead, the temperature of transformation seems to be inversely dependent on the level of structural imperfections of the solid, as evaluated by the values of crystallite size and lattice strains, computed by X-ray diffraction line broadening analysis.

This paper describes complementary results on the thermal stability of various $\gamma\text{-Fe}_2\text{O}_3$ samples obtained by five completely different synthetic routes.

EXPERIMENTAL

Four samples of $\gamma\text{-Fe}_2\text{O}_3$ -named A, B, C and D- were obtained by thermal decomposition of the following compounds: $\gamma\text{-FeOOH}$, $\alpha\text{-FeOOH}$, $\text{N}_2\text{H}_5\text{Fe}(\text{N}_2\text{H}_3\text{-COO})_3 \cdot \text{H}_2\text{O}$ [6], and FeOOCH_3 [7], respectively. For sample B, the ex- $\alpha\text{-FeOOH}$ haematite was reduced by hydrogen at 315 °C and the resulting Fe_3O_4 was oxidized in air atmosphere at 250°C. Sample E was an iron oxide colloid and its preparation was carried out by the procedure described in ref. [8].

The measurements of specific surface area were carried out by the BET method using nitrogen. The thermal analysis curves were recorded on different instruments under static air atmosphere: Setaram TA 24, Stanton Redcroft 670-3, Mettler TA 3000 and Rigaku BPS1. The XRD patterns were obtained with a Siemens diffractometer D500 using CuK_α radiation monochromated by a graphite crystal. XRD line broadening analysis was performed by the procedure already described [5].

RESULTS AND DISCUSSION

X-ray diffraction data and chemical analysis of Fe(II) showed that all samples were $\gamma\text{-Fe}_2\text{O}_3$ of high purity, with the exception of sample E in which an amount of Fe(II) of approximately 2 % was found. Some structural and textural properties of the samples, which will be discussed below are collected in Table 1.

Four samples showed a narrow distribution both in the size and the shape of the particles (Fig. 1). However, the particles of sample D show a broad size distribution and an irregular morphology. Electron micrographs suggest that these particles are built up of a mosaic of many crystallites.

The DTA traces of some selected samples are included in Fig. 2, the shape of the $\gamma\text{-Fe}_2\text{O}_3$ to $\alpha\text{-Fe}_2\text{O}_3$ exothermic transformation was variable, as found in previous reports [2,5,8].

Ravindranathan et al. [6] have reported that the conversion of $\gamma\text{-Fe}_2\text{O}_3$ to $\alpha\text{-Fe}_2\text{O}_3$ takes place at 595°C and is characterized by a sharp exothermic peak. In the present study, these results are only partially confirmed, if the thermodifferential curve is recorded in a Stanton Redcroft apparatus, in which the sample is compacted within the container. Under these conditions, the DTA curve is that shown in Fig. 2a. The broad exothermic effect located at 400°C is due to a partial transformation of $\gamma\text{-Fe}_2\text{O}_3$ to $\alpha\text{-Fe}_2\text{O}_3$. The composition evaluated from XRD data yields a value of 35 % in $\alpha\text{-Fe}_2\text{O}_3$. At the end of the sharp exotherm the product is monophasic by XRD, but the most relevant feature is the sintering of the haematite particles that leads to a 94 % decrease in the

TABLE 1

Values of different parameters obtained from XRD patterns and DTA curves for $\gamma\text{-Fe}_2\text{O}_3$ samples. Values of specific surface area have also been included.

Sample	FWHM($^\circ$)*	β ($^\circ$)**	ϵ (\AA)**	$\bar{\epsilon} \cdot 10^3$ **	S_{BET} ($\text{m}^2 \text{g}^{-1}$)	T_p ($^\circ\text{C}$)
A	1.686 1.369	2.352	55	13.1	109	400
B	0.252 0.344	0.316	2224	0.2	20	550
C	1.035 1.255	1.402	108	8.9	150	550
D	0.643 0.745	0.788	401	6.8	71	540
E	1.019 1.010	1.243	220	11.4	116	505

* Full width at half maximum for 313 and 440 lines.

**Values referred to the 313 reflection.

β Integral breadth

ϵ Volume-averaged crystallite size.

$\bar{\epsilon}$ microstrains.

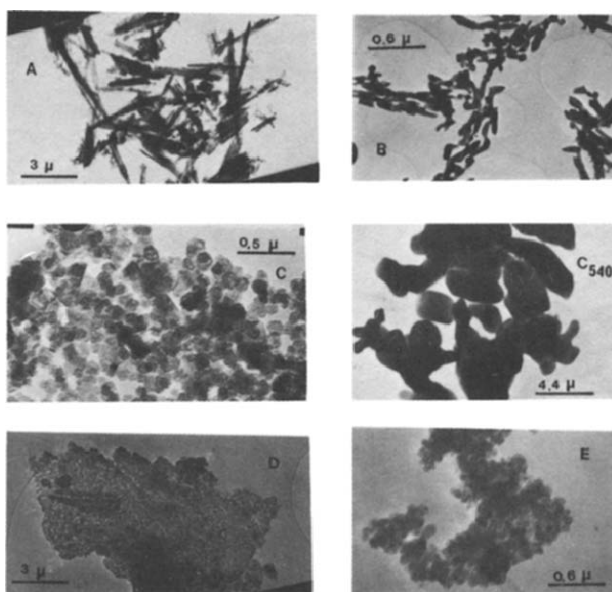


Fig. 1. Electron micrographs of the different samples of $\gamma\text{-Fe}_2\text{O}_3$. The micrograph C540 corresponds to sample C heated at 540°C in a Stanton Redcroft DTA apparatus.

specific surface area. The larger size of haematite particles relative to the initial maghemite crystal is also shown in the results obtained from the profile broadening analysis summarized in Table 2. Moreover, preferential X-ray line broadening, which is usually observed in haematite derived from the thermal decomposition of hydroxy compounds [9] is absent in this sample. This fact is indicative of a regular growth of initial nuclei of haematite that results in an isotropic shape of the coherently diffracting haematite domains, similar to that found in a high temperature treated haematite.

When the ATD of this sample is recorded in a Setaran or a Rigaku apparatus in which the sample is uncompressed in the holder, a broad and diffuse exotherm characterizes the phase transition. Thus, only when the contact between particles is facilitated, the fast sintering process dominates the release of heat and the shape of the peak is similar to the aspects of the "glow phenomena" observed in other materials [10]. Other samples, particularly those of acicular morphology did not show this exceptional behaviour, whatever the apparatus used for recording the DTA curve (see Fig. 2). An intermediate situation is shown by sample E. Even for this sample, which shows the smaller particle size, the DTA curve recorded in Setaram yields a well-defined peak.

These results can be summarized as follows. In those samples of ultrafine texture with particles of plate morphology, the main contribution to the sharp exotherm appears to be the sintering of particles, since this morphology allows a good contact between particles. In contrast, these favourable conditions are not found for an acicular morphology. Previous results have shown that when $\text{ex-}\gamma\text{-FeOOH}$ $\gamma\text{-Fe}_2\text{O}_3$ is completely transformed into haematite, the particles maintain a porous texture although a decrease in the BET surface is detected [5]. For this type of sample, the profiles of the exothermal peak are mainly controlled by the heat evolved in the transformation and its sluggish character is reflected as a broad and diffuse signal.

A logical consequence of these considerations is the absence of a clear relationship between the specific surface area and the temperature of the peak (see Table 1). These results are in contrast with the commonly accepted conclusion that the temperature of transformation is inversely related to particle size [1-5].

With the exception of sample C, which possesses an overall more complex thermal behaviour. An increase is noted in the rate of transformation with the increase of the broadness of the XRD line profiles (see Table 1). Thus, the reduction in the size of coherently diffracting domains within particles, accompanied by an increase in the distortion given by the lattice strains ϵ , unstabilizes $\gamma\text{-Fe}_2\text{O}_3$ with respect to its transformation. Presumably, this high degree of disorder helps the shearing process necessary to change the

TABLE 2

Crystallite size and lattice strains obtained from XRD line broadening analysis of different profiles of $\gamma\text{-Fe}_2\text{O}_3$ and $\alpha\text{-Fe}_2\text{O}_3$. These data correspond to sample C and the thermal treatments were carried out in the Stanto Redcroft DTA apparatus.

Sample	line	$\beta^{\circ}2\theta$	$\epsilon^{\circ}(\text{\AA})$	$\bar{\epsilon} (.10^3)$
Unheated	220	0.798	364	6.4
	400	0.810	489	4.6
T=420°C	220	0.776	399	6.4
	400	0.808	432	4.7
	**104	0.332	1168	1.8
	**024	0.397	827	0.9
T=540°C	**104	0.257	2116	0.7
	**024	0.315	1762	0.2

** Reflections belonging to $\alpha\text{-Fe}_2\text{O}_3$.

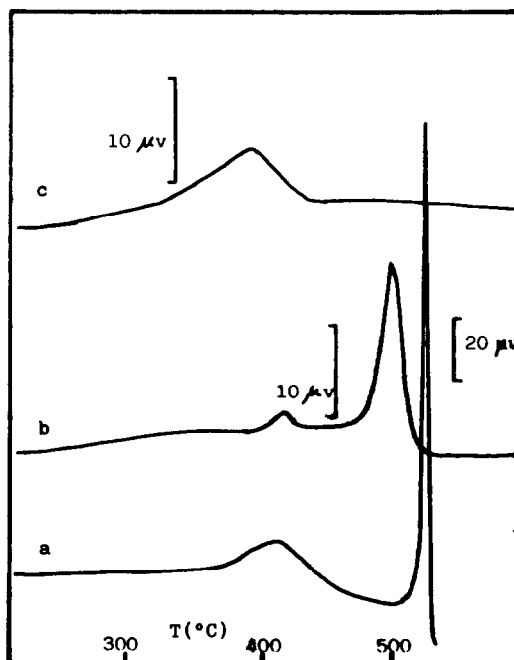


Fig. 2. DTA curves of some selected samples of $\gamma\text{-Fe}_2\text{O}_3$: Curve a corresponds to sample C (weight: 52.4 mg) and was recorded in a Stanton Redcroft apparatus. Curves b and c correspond to samples E (26.8 mg) and A (13.8 mg) respectively and were recorded in a Setaram TAG-24 system.

stacking sequence of oxygen layers from cubic to hexagonal closest packing. The transformation also involves a migration of Fe^{+3} from tetrahedral to octahedral holes. It seems obvious that such a movement can be facilitated within a lattice of high $\tilde{\epsilon}$, which is equivalent to having a low degree of crystallinity. Of course, this is only one of the factors that affects the stabilization of $\gamma\text{-Fe}_2\text{O}_3$, which has also been understood in terms of protons occupying some vacancies and/or the participation of hydroxyl groups [11].

ACKNOWLEDGEMENT

This work was carried out with the financial support of CAICYT (contract 0982-84).

REFERENCES

- 1 A. Rousset, G. Boissier, J.P. Caffin and F. Cassagneux, C.R. Acad. Sc. Paris, 299 (1984) 781.
- 2 A.C. Vajpei, F. Mathieu, A. Rousset, F. Chasagneux, J.M. Letoffe and P. Claudy, J. Thermal Anal. 32 (1987) 857.
- 3 C. Sarda, F. Mathieu, A.C. Vajpei and A. Rousset, J. Thermal Anal. 32 (1987) 865.
- 4 F. Mathieu, P. Roux, G. Bonel and A. Rousset, C.R. Acad. Sci. Paris, 305 (1987) 249.
- 5 R. Gómez-Villacieros, L. Hernán, J. Morales and J.L. Tirado, Mat. Res. Bull. 22 (1987) 513.
- 6 P. Ravindranathan and K.C. Patil, J. Mater. Sci. Lett. 5 (1986) 221.
- 7 S. Kikkawa, F. Kanamaru and M. Koizumi, Inorg. Chem. 15 (1976) 2195.
- 8 E. Tronc, J.P. Jolivet and J. Livage, J. Chem. Res. (1987) 136.
- 9 J.M. Jiménez-Mateos, J. Morales and J.L. Tirado, J. Mater. Sci. Lett. 5 (1986) 1295.
- 10 M.A. Alario-Franco, J. Fenerty and K.S.W. Sing, Proc. 7th Int. Symp. Reactiv. Solids, (1972) 327.
- 11 P.B. Braun, Nature, 170 (1952) 1123.